

# Enhanced Ferroelectric and Dielectric Properties in $\text{Bi}_{0.5}\text{Na}_{0.5}\text{TiO}_3$ Doped with $\text{BaTiO}_3$ (BNT-BT) Nanoparticles for High Energy Storage Device

Manju Kumari, Neeraj Dhariwal, Preeti Yadav, Vinod Kumar, & O P Thakur\*

Materials Analysis & Research Laboratory, Department of Physics, Netaji Subhas University of Technology, New Delhi 110 078, India

Received: 9 August 2023; Accepted: 26 September 2023

Nanoparticles of lead-free  $\text{Bi}_{0.5}\text{Na}_{0.5}\text{TiO}_3$  doped with  $\text{BaTiO}_3$  (BNT-BT) have been fabricated by the auto-combustion sol-gel method. A structural and morphological analysis of the developed material has been performed by using XRD and FESEM. Also, a temperature and frequency (100Hz-1MHz) dependent dielectric study of BNT-BT nanoparticles has been conducted, resulting in a variation that occurs at  $120.83^\circ\text{C}$  due to transition from ferroelectric to antiferroelectric phase, followed by a sudden increase due to paraelectric phase formation. Additionally, as frequency increased, the dielectric constant decreased exhibiting Maxwell-Wagner polarization. The ferroelectric study has been done by using PE loop at room temperature ( $28^\circ\text{C}$ ). The maximum value obtained for remanent polarization and saturation polarization is  $1.73\ \mu\text{C}/\text{cm}^2$  and  $3.75\ \mu\text{C}/\text{cm}^2$  respectively at an applied electric field of  $28\ \text{kV}/\text{cm}$ . The value for the recoverable energy storage density ( $W_1$ ) is  $0.0483\ \text{J}/\text{cm}^3$ , energy loss density ( $W_2$ ) is  $0.05378\ \text{J}/\text{cm}^3$  and its efficiency ( $\Gamma$ ) is 47% at an applied field  $28\ \text{kV}/\text{cm}$ . The obtained results for the BNT-BT nanoparticles are remarkable for energy storage devices, and they further indicate their potential for energy harvesting and high piezoelectric sensors for industrial purposes.

**Keywords:** Dielectric, Energy Storage, Ferroelectric, Nanoparticles, Polarization

## 1 Introduction

Over the past few decades, there has been a trend of exploring and building industrialization to improve mankind's things, such as energy storage devices for utilizing energy<sup>1</sup>. For this, there is excess use of lead-based materials such as  $\text{Pb}(\text{Zr},\text{Ti})\text{O}_3$ ,  $\text{PbTiO}_3$ ,  $\text{Pb}(\text{MgNb})\text{O}_3$ , because of their attractive properties like excellent electromechanical, high coupling factors and piezoelectric coefficient<sup>2,3</sup>, but recently due to the toxicity and hazardous nature of these materials legislation has been passed by the European Union to restrict the use of lead-based materials. Lead-free piezoelectric materials such as Bismuth Sodium Titanate i.e. ( $\text{Bi}_{0.5}\text{Na}_{0.5}\text{TiO}_3$ ; BNT) are considered one of the best replacement materials for lead-based ceramics for energy storage and memory devices<sup>4</sup>. Despite its large conductivity and high coercive field, pure BNT ceramics are difficult to pole. Hence, Barium Titanate ( $\text{BaTiO}_3$ ; BT) phase was added into pure BNT ceramics to modify their electrical properties<sup>5</sup>. A number of studies have been conducted on Barium Titanate (BT;  $\text{BaTiO}_3$ ), which is a lead-free ceramic with good electrical properties and strong ferroelectric properties<sup>6</sup>. It has a high dielectric

constant, polarization level, controllable loss, and low toxicity character. In the literature, a lot of studies are being conducted on lead-free materials that based on bismuth sodium titanate and barium titanate, such as, BNT-ST, 0.70BLNBT-0.30STN and BNT-KNN<sup>7-9</sup>.

In this study, we synthesized a lead-free piezoelectric material i.e.,  $\text{Bi}_{0.5}\text{Na}_{0.5}\text{TiO}_3$  doped with  $\text{BaTiO}_3$  (BNT-BT) by auto-combustion sol gel method. This paper investigates the microstructure, dielectric and ferroelectric properties of the material. The developed material improves the dielectric and ferroelectric properties by specifying the material composition, which are useful properties for energy storage device applications.

## 2 Materials and Method

$(1-x)\text{Bi}_{0.5}\text{Na}_{0.5}\text{TiO}_3 - x\text{BaTiO}_3$  where  $x=0.08$  i.e.  $\text{Bi}_{0.5}\text{Na}_{0.5}\text{TiO}_3$  doped with  $\text{BaTiO}_3$  (BNT-BT) was synthesized by auto-combustion sol gel technique as shown in Fig. 1. In this investigation, high purity salts of  $\text{Bi}(\text{CH}_3\text{COO})$ ,  $\text{C}_2\text{H}_3\text{NaO}_2$ ,  $\text{C}_4\text{H}_6\text{BaO}_4$  and  $\text{C}_{12}\text{H}_{28}\text{O}_4\text{Ti}$  were employed as the raw materials. Firstly,  $\text{Bi}(\text{CH}_3\text{COO})$  was dissolved at  $100^\circ\text{C}$  in acetic acid for 1 h and simultaneously  $\text{C}_2\text{H}_3\text{NaO}_2$  and  $\text{C}_4\text{H}_6\text{BaO}_4$  were dissolved in D.I water for 30 mins while  $\text{C}_{12}\text{H}_{28}\text{O}_4\text{Ti}$  dissolved for 1 h in ethanol. By

\*Corresponding author (E-mail: ophthakur@nsut.ac.in)

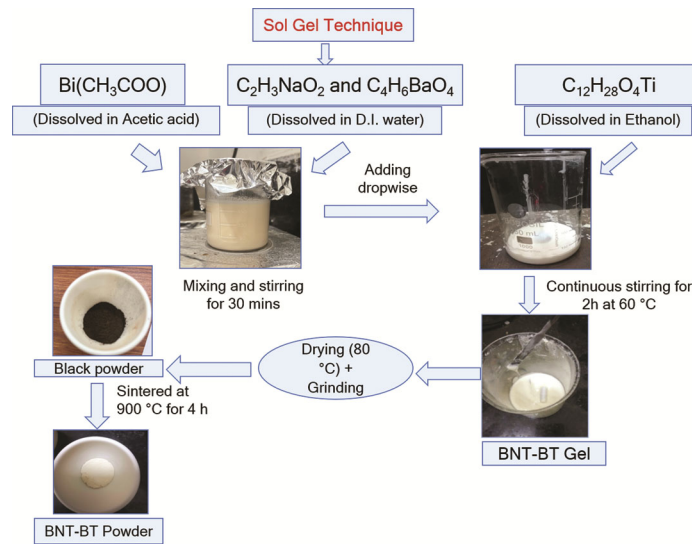


Fig. 1 — Flow chart of the BNT-BT synthesis of nanoparticles.

continuous stirring, all dissolved solutions were mixed, and further after adding citric acid, the solution was stirred for 2 h at 60 °C until BNT-BT gel was obtained. BNT-BT gel was dried at 80 °C and then ground in a mortar pestle to obtain a powder. Finally, after sintering at 900 °C for 4 h, the BNT-BT powder (white yellow) was obtained.

### 2.1 Characterization Techniques Used

Structural and morphological study were done by XRD and FESEM, while electrical properties such as dielectric study and ferroelectric study measurement were done by LCR meter and PE loop set up respectively.

## 3 Result and Discussion

Figure 2 depicts the XRD pattern of the BNT-BT nanoparticles that includes the all peaks of the prepared material. The formation of crystalline structure was confirmed by the JCPDS file. Both the phases of BNT and BT nanoparticles are present in the XRD graph. As shown in XRD graph, there is a formation of secondary phase at 30° as represented by \*, which is due to high heat treatment.  $\text{Bi}_2\text{O}_3$  phase is losing their appearance, and there is formation of small secondary phase as represented as  $\text{Na}_{0.5}\text{Ti}_4\text{Bi}_{4.5}\text{O}_{15}$  which is also confirmed from the JCPDS no (74-1319)<sup>10</sup>.

The FESEM micrograph of the BNT-BT material was depicted in Fig. 3, that represent as a pebble like structure. Clearly, the FESEM image of BNT-BT nanomaterials shows dense uniform structures that confirms the homogeneity of the materials. Also, the

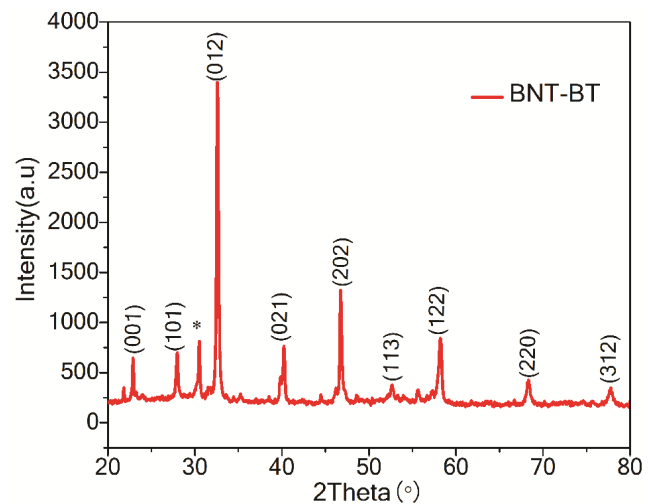


Fig. 2 —XRD pattern of BNT-BT nanomaterials.

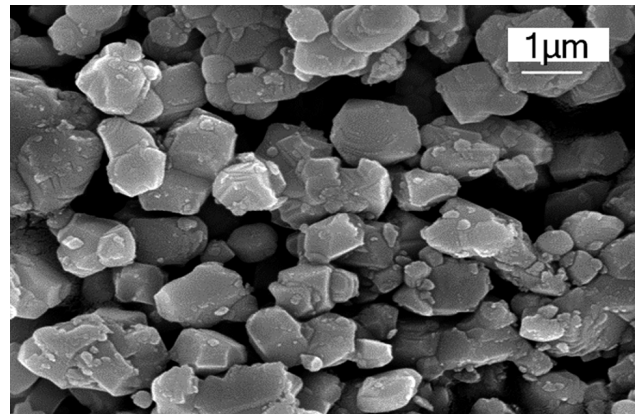


Fig. 3 — FESEM image of BNT-BT nanomaterials.

grain boundaries appear to be clear, with less porosity.

Figure 4 exhibits the variation of dielectric constant (permittivity) w.r.t temperature for different frequencies, and dielectric constant vs frequency for different temperature. At low temperature and low frequency, the dielectric constant value is very high. The dielectric constant value is around 1000 at 1 KHz while it starts decreasing with increase in frequency. This exhibited behavior was clearly explained by Maxwell Wagner theory of interfacial polarization<sup>11</sup>. An anti-ferroelectric phase transition occurs at the

Depolarization temperature (120.83 °C) when a ferroelectric phase transitions to an anti-ferroelectric phase. Also, at high temperature, there is minor fluctuations and there is sudden increase in dielectric constant value because of further appearance of second phase transition, that is, from anti ferroelectric phase to paraelectric phase<sup>12</sup>.

As shown in Fig. 5, the PE loop study of the BNT-BT nanomaterials shows the maximum value of remnant polarization  $P_r = 1.73 \mu\text{C}/\text{cm}^2$  and saturation polarization  $P_s = 3.75 \mu\text{C}/\text{cm}^2$  for an applied field

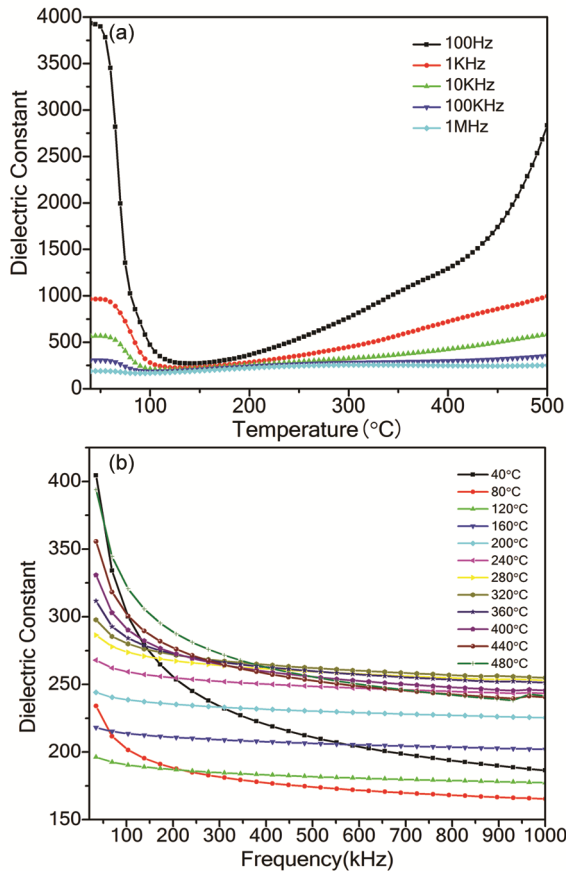


Fig. 4 — (a-b) Depicted the variation of dielectric constant ( $\epsilon'$ ) with temperature for different frequencies and dielectric constant with frequency for different temperature.

28 kV/cm, In turn, this facilitates energy storage density. PE loops are beneficial in the calculation of the parameters such as the recoverable energy storage density ( $W_1$ ), energy loss density ( $W_2$ ) and efficiency ( $\eta$ ) of the material<sup>13</sup>. For this calculation, the following equations are used<sup>14</sup>:

$$W_1 = \int_{P_r}^{P_{max}} E dp, \quad \dots (1)$$

$$\eta = \frac{W_1}{W_1 + W_2} \quad \dots (2)$$

The obtained value for the recoverable energy storage density ( $W_1$ ) is  $0.0483 \text{ J}/\text{cm}^3$ , energy loss density ( $W_2$ ) is  $0.05378 \text{ J}/\text{cm}^3$  (see Fig. 6) and its efficiency ( $\eta$ ) is 47% at an applied field of 28 kV/cm. It is clear that the obtained value of energy storage density at a low electric field is good and it should

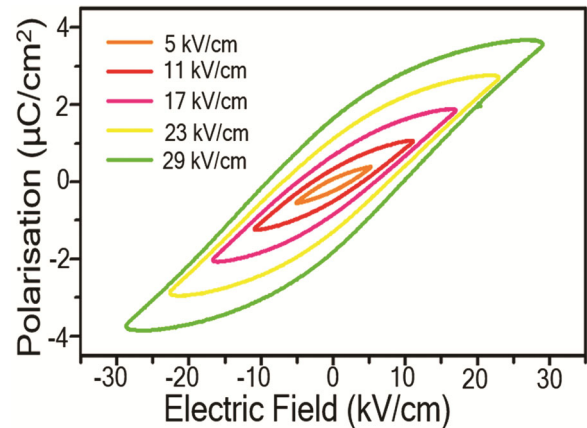


Fig. 5 — Polarization versus Electric Field measurement at an applied field 5-30 kV/cm

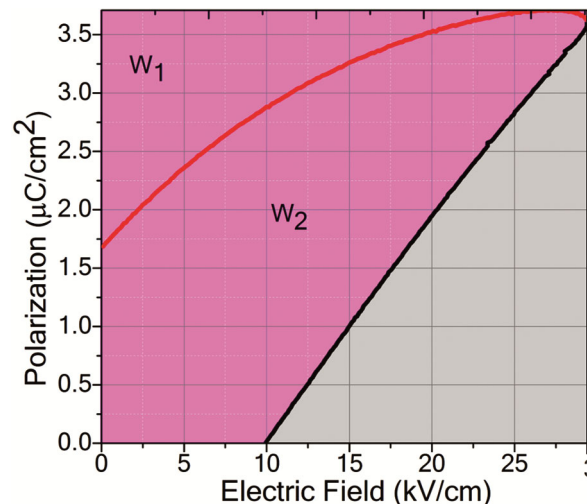


Fig. 6 — Area enclosed by recoverable energy storage density ( $W_1$ ) and energy loss density ( $W_2$ ) for an electric field of 28 kV/cm.

contribute to the formation of storage devices, but because of the limitations of our setup for the requirement of higher applied electric field, the energy storage density value is lower than its possible higher value which can be obtained when electric field gets increased. So, if there is a chance of increasing the electric field, the polarization value increases which enhances the energy storage capacity of the material.

#### 4 Conclusion

In this paper, the energy storage property of lead free  $\text{Bi}_{0.5}\text{Na}_{0.5}\text{TiO}_3$  doped with  $\text{BaTiO}_3$  (BNT-BT) nanoparticles have been studied which was fabricated by using auto combustion sol gel method. XRD pattern confirms the proper phase formation of the obtained BNT-BT nanoparticles. FESEM image clearly shows dense uniform structures that confirm the homogeneity of the materials. The temperature and frequency dependent dielectric properties of synthesized BNT-BT nanoparticles exhibit the transition of ferroelectric phase to an antiferroelectric at depolarization temperature i.e., 120.83 °C. There is minor dielectric dispersion and a sudden increase in the value of the dielectric constant due to further paraelectric transition. PE loop study reveals the energy storage density of the developed nanomaterials. The remanent polarization and saturation polarization are the key factors, which were found to be  $P_r = 1.73 \mu\text{C}/\text{cm}^2$  and  $P_s = 3.75 \mu\text{C}/\text{cm}^2$  at an applied field of 28 kV/cm. Also, the value of recoverable energy storage density ( $W_1$ ) is  $0.0483 \text{ J}/\text{cm}^3$ , energy loss density ( $W_2$ ) is  $0.05378 \text{ J}/\text{cm}^3$  and its efficiency ( $\eta$ ) is 47%. Thus, the results obtained

from this study confirms the excellent property of lead free BNT-BT nanoparticles that are notable for energy storage devices. Also, it is beneficial in electronic gadgets, and it has the potential for energy harvesting and high piezoelectric sensors for industrial purposes.

#### References

- 1 Yao Z, Song Z, Hao H, Yu Z, Cao M, Zhang S, Lanagan M T & Liu H, *Adv Materials*, (2017) 1601727.
- 2 Yu Z, Yang J, Cao J, Bian L, Li Z, Yuan X, Wang Z, Li Q and Dong S, *Adv Functional Materials*, 32(25) (2022) 2111140.
- 3 Wang P, Guo Q, Li F, Xia F, Hao H, Sun H, Liu H and Zhang S, *J American Ceramic Society*, 104(10) (2021) 5127.
- 4 Panda P K & Sahoo B, *PZT to lead free piezo ceramics: a review*, *Ferroelectrics*, 474 (2015).
- 5 Li L, Hao J, Xu Z, Li W & Chu R, *Materials letters*, 184 (2016) 152.
- 6 Alkathy MS & Raju, KJ, *J Magnetism and Magnetic Materials*, 452 (2018) 40.
- 7 Cao W.P Li WL, Dai XF, Zhang TD, Sheng, J, Hou YF & Fei W.D, *J European Ceramic Society*, 36(3) (2016) 593.
- 8 Wu L, Tang L, Zhai Y, Zhang Y, Sun J, Hu D, Pan Z, Su Z, Zhang Y and Liu J, *J Materiomics*, 8(3) (2022) 537.
- 9 Hao J, Xu Z, Chu R, Li W, Juan D. & Peng F *Solid State Communications*, 204 (2015) 19.
- 10 Wu W, Han Y, Huang X, Du J, Bai W, Wen, F, Wu W, Zheng P, Zheng L and Zhang Y, *J Australian Ceramic Society*, 57 (2021) 321.
- 11 Kumari M, Chahar M, Shankar S. and Thakur OP, *Materials Today: Proceedings*, 67 (2022) 688.
- 12 Jin CC, Wang FF, Wei LL, Tang J, Li Y, Yao QR, Tian CY & Shi W.Z, *J alloys and compounds*, 585 (2014) 185.
- 13 Wang D, Fan Z, Li W, Zhou D, Feteira A, Wang G, Murakami S, Sun S, Zhao Q, Tan X & Reaney IM, *ACS Applied Energy Materials*, 1(8) (2018) 4403.
- 14 Ma W, Zhu Y, Marwat MA, Fan P, Xie B, Salamon D, Ye ZG & Zhang H, *J Materials Chemistry C*, 7(2) (2019) 281.